International Symposium COMODIA 90: 59-64(1990)

Prediction of Unburned Gas Temperature in Multidimensional Engine Combustion Simulation

A.D.Gosman, C.J.Marooney and H.G.Weller

Mechanical Engineering Department
Imperial College
Exhibition Road
London SW7 2BX
U.K.

ABSTRACT

The prediction of flame propagation and knock in reciprocating engines requires knowledge of the temperature distribution in the unburned gases ahead of the flame. This is conventionally obtained in ensemble-averaged multidimensional representations of the combustion processes from the predicted ensemble-mean enthalpy and species concentration fields. In some cases the estimate is refined with the aid of presumptions about the form of the scalar p.d.f. Since however combustion usually occurs in the 'laminar flamelet' regime, where the burnt and unburned gases are separated by a thin flamefront, the former practice can lead to a substantial overestimate of the unburned gas temperature while the latter will yield a substantial underestimate when, as is invariably the case, appreciable wall heat losses occur. These errors can produce, on the one hand erroneous values of the laminar flame properties which are used in some combustion models, and on the other the need to introduce artifical temperature limits in the calculation of knock-producing reactions.

The present paper describes a novel modelled transport equation of the scalar properties of the unburned gas which explicitly recognises the existence of the sharp burned/unburned gas interface and thereby produces more realistic values for the unburned temperature. The utility of the model is demonstrated by comparative calculations of knock using the conventional and newly-developed approaches.

1. INTRODUCTION

Recent advances in homogeneous-charge combustion modelling [1-6] have been based on the laminar-flamelet concept, in which the details of the chemistry are subsumed in a single parameter, the laminar flame speed, which is correlated against pressure and temperature. Since the correlation refers to conditions in the unburnt gas into which the flame propagates, it is important to distinguish the unburnt gas conditions from those calculated using the ensemble-averaged equations conventionally used in engine simulations; however, the unburnt gas values cannot be evaluated solely from a knowledge of the ensemble-averaged values. Similar considerations apply to the low-temperature chemistry of autoignition, whether in Diesel ignition, or knock in spark-ignited engines. Here, the concentrations of the radical species, as well as the temperature, must be evaluated in the unburnt phase for the autoignition kinetics, on the assumption that the presence of the flame will suppress the self-catalysing nature of this chemistry.

Previous attempts to predict knock in spark ignition engines by calculating the flow field and combustion have highlighted the limitations of the traditional ensemble average approach [7], in which interaction between the low-temperature kinetics and the flame calculations causes accelerated flame propagation and premature knock. The interaction problem has been addressed by Natarajan et.al. [8,9] in which either the low-temperature kinetics calculations are switched off in regions of rapid combustion, or an extra radical is added to the system which effectively damps the interaction. This latter technique is applicable to codes in which the flame is represented by a kinetic scheme, but not to those in which the ensemble average turbulent flame front is considered as a probability distribution of a laminar front, or derived from a turbulent mixing model.

By contrast, good knock simulations have been produced by considering the unburnt and burnt gases independently, separated by an infinitely thin flame, in the zero-dimensional engine calculations of Hirst et al [10], within the limitations of the assumption of spatial uniformity for the two gas phases. In this paper we develop equations for the three-dimensional evolution of these two gas-phase fields, within the context of ensemble- averaged calculations. The general theory is set out in the next section. It is intended to apply in the laminar flamelet combustion regime, and so is more germane to spark-ignition engines, although some phases of Diesel combustion also fall in this regime.

To illustrate the applications of the theory, calculations of the onset of knock in a homogeneous-charge spark-ignition engine with 4-valve pent-roof geometry are presented in section 3. These show clearly the improvement obtained in using unburnt-phase equations, not only in the prediction of knock but also in reproducing observed details of knock phenomenology.

2. TWO-PHASE COMBUSTION THEORY

Within the laminar flamelet regime in homogeneous combustion, the system can be divided into two phases of burnt and unburnt gas, separated by a thin reaction zone. This zone propagates into the unburnt gas at a local speed $S_u(T_u, P, f_u)$, the laminar flame speed at unburnt gas temperature T_u, pressure P and fuel concentration f_u. Although S_u is also a function of the flame strain, this effect will not be further considered in this study. The low-temperature reactions in the unburnt phase lead to radical production causing the temperature to rise with an associated increase in flame-speed. It is assumed that this effect is given in the temperature dependence of S_u, and that no further acceleration of the flame due to the radicals need be modelled. The low-temperature reactions are thus assumed in the model to be suppressed at the flame-front, which is not directly affected by them [11,12].

On the basis of the forgoing assumptions, two-phase modelling techniques, in which the phases are separated by a thin interface, may be applied to flame propagation, the only difference being that in this case the interface propagates. In general this approach would require that the velocity and pressure of the two phases be independently calculated including the slip between phases. However a single velocity and pressure will nonetheless usually suffice to characterize both phases, if they are well interspersed by the flame wrinkling at the discretization length-scales of the calculation mesh. This considerably simplifies a problem already made complex by the addition of the fields for the radicals in the autoignition kinetics, and appears to be justified by the success of predictions made with this approximation. This also means that only one set of turbulence parameters is used. However, the volume dilations, and hence the divergence of velocity, of the two phases are very different, but can be obtained from thermodynamic considerations, as will be shown.

(a) Transport Equations

From these considerations, the transport equation for a scalar field in the unburnt phase can be derived to be

$$\frac{\partial \rho [m_u \psi_u]}{\partial t} + \nabla \cdot (\rho \mathbf{U}[m_u \psi_u]) - \nabla \cdot (\rho m_u D_\psi \nabla \psi_u) = \rho [m_u \dot{\psi}_u] + \rho [\dot{m}_u \psi_u] \qquad (1)$$

where subscript u denotes the unburnt phase, m is the phase mass fraction, ρ is the phase average density, D_ψ is the molecular diffusivity and a superposed dot denotes the reaction rate. ψ is a member of the set $\{1, R_i, f, e\}$, with f the fuel concentration, R_i the set of autoignition radicals, and e the internal energy. For $\psi=1$ (the mass transport equation) $D_\psi=0$. The first term in this equation represents the rate of change of the unburnt gas property due to all processes, transport, diffusive and source. The second represents convection of the property. The third, molecular diffusion, term only represents diffusion within the unburnt-phase, as diffusional transport within the flame is effectively included through the laminar flame speed. The two right-hand-side terms are the unburnt gas property souce and flame propagation unburnt gas consumption rate source terms respectively.

The instantaneous equation can be replaced by a Favre-averaged one of exactly the same form [16, 17], by noting first that the fluctuations in m_u about the Favre-average, m_u'', represent fluctuations in the flame-front position due to turbulence/flame interaction, while ψ_u'' denotes fluctuations of the unburnt gas property due to turbulence/property gradient interaction: these are uncorrelated, so that $\widetilde{m_u \psi_u} = \widetilde{m_u}\widetilde{\psi_u}$. After this, the triple correlation term $\widetilde{m_u'' \psi_u'' U''}$ is assumed small in comparison with the double correlation terms because fluctuations of ψ_u are considered small compared with those of m_u due to the small concentration gradients expected for $\widetilde{\psi_u}$, and uncorrelated. Finally the Boussinesq approximation replaces double correlation terms in $\widetilde{U'' m_u''}$ *and* $\widetilde{U'' \psi_u''}$ by eddy diffusivity transport terms, with D_ψ replaced by Γ_ψ the total (turbulent plus molecular) diffusivity. The assumption that the unburnt gas property concentration and flame position are uncorrelated then allows the unburnt mass fraction to be related to the fuel concentrations (subscript b for the burnt phase) through

$$\tilde{m}_u = \frac{\tilde{f} - \tilde{f}_b}{\tilde{f}_u - \tilde{f}_b} \qquad (2)$$

(b) Combustion Model

For this study, we choose the Magnussen model [13] for the ensemble-average consumption rate on account of its simplicity; in the expectation, to be justified in the results, that the description of the unburnt phase given above gives the important features of the effect of a two-phase system on flame propagation and knock. However, there is a problem in implementing this model in the standard form for it gives the reaction rate as

$$\dot{f} = -\frac{A}{\tau}\min\left(M_{fuel}, M_{oxidant}, BM_{products}\right) \quad (3)$$

where M is the species mass fraction, and A and B are the Magnussen model coefficients [13], taken as 16.0 and 0.5 respectively in the present work.

This expression is inappropriate when used in conjunction with low temperature kinetics calculations, whose product generation would promote the flame propagation rate. The solution is to use a mass based progress variable c (equivalent to $1\text{-}m_u$) since, following the above discussion, m_u represents only the movement of the flame-front and does not include autoignition chemistry. Further, since the unburnt fuel distribution is inhomogeneous, we need to define a local progress variable

$$\tilde{c} = (\tilde{f}_u - \tilde{f}) / (\tilde{f}_u - \tilde{f}_b) \quad (4)$$

The modified Magnussen reaction rate expression is then

$$\dot{m}_u = -\frac{A}{\tau}\min(1 - \tilde{c}, B\tilde{c}) \quad (5)$$

(c). Energy Equation

In the transport equation for the unburnt-phase internal energy, the compression work is represented by

$$\tilde{m}_u \frac{\bar{\rho}}{\bar{\rho}_u} P \nabla \cdot \tilde{\mathbf{u}}_u \quad (6)$$

with $\widetilde{m}_u\bar{\rho}/\bar{\rho}_u$ the fractional volume of the unburnt phase. Using

$$\nabla \cdot \tilde{\mathbf{U}}_u = -\frac{1}{\bar{\rho}_u}\left(\frac{\partial \bar{\rho}_u}{\partial t}\right)_{m_u} \quad (7)$$

where the subscript m_u denotes differentiation at constant flame position, this term becomes

$$\tilde{m}_u \frac{\bar{\rho}}{\bar{\rho}_u}\left(\frac{\partial P}{\partial t} - \frac{P}{T_u}\frac{\partial \tilde{T}_u}{\partial t}\right)_{m_u} \quad (8)$$

The wall heat transfer is given by the law of the wall as the product of heat transfer coefficient, wall contact area for unburnt phase, and unburnt energy normal gradient. The fractional area of the unburnt phase in contact with the wall is assumed the same as its volume fraction, consistent with the assumption that the two phases are well interspersed.

(d). Calculation

The unburnt-phase transport equations can be integrated computationally in the same manner as their conventional ensemble-average counterparts, yielding a solution for $\widetilde{m_u\psi_u}$. Solution of the fuel concentration (or equivalently the progress variable) then gives $\widetilde{m_u}$ and consequently $\widetilde{\psi_u}$. However, this solution method becomes ill-posed in nearly-burnt regions, where $\widetilde{m_u}$ approaches zero; an effect produced by the finite tolerance on the numerical solution of $\widetilde{m_u\psi_u}$. This has an obvious physical meaning: unburnt-state quantities are not defined when the unburnt phase is not present. However, in an ensemble-average flame calculation, the flame does exist with some probability at all points and it is necessary to define its unburnt gas temperature as input to the flame-speed correlation. For these reasons, it is desirable to solve an equation directly for $\widetilde{\psi_u}$. This equation can be derived by multiplying the unburnt mass transport equation by $\widetilde{\psi_u}$ and subtracting the result from equation (1) for $\widetilde{m_u\psi_u}$ to yield

$$\bar{\rho}\frac{\partial \tilde{\psi}_u}{\partial t} + \left\{\bar{\rho}\tilde{\mathbf{U}} - 2\Gamma_\psi \frac{\nabla \tilde{m}_u}{\tilde{m}_u}\right\} \cdot \nabla\tilde{\psi}_u - \nabla \cdot \left(\Gamma_\psi \nabla \tilde{\psi}_u\right) = \bar{\rho}\dot{\psi}_u \quad (9)$$

It will be seen from this that the fluctuations of the flamefront contribute a net additional mean velocity seen by the ensemble unburnt gas property.

One further advantage of equation (9) is that its source terms do not contain the combustion due to flame front propagation. Provided $\widetilde{m_u}^{-1}$—$\widetilde{m_u}$ remains bounded in the limit $\widetilde{m_u}\text{->}0$, the equation is stable, and can also be easily solved numerically in conjunction with the ensemble-averaged system. However, the system as presented may not yield nearly-equal unburnt and ensemble temperatures far from the flamefront, due to the differences in the discretization of the two equations; this can be avoided by deriving the discrete version of the equation as the difference of the equivalent parent discretized equations.

3. ASSESSMENT OF METHOD

The two alternatives to the present method of unburnt gas calculation which are currently used in practical knock calculations are (a) to use only total ensemble-averaged properties, and solve for both low-temperature kinetics and high-temperature flame propagation [7], or (b) use total properties, and assign an interface criterion which switches off the low-temperature kinetics in regions of rapid combustion [8,9]. To compare our method with these alternatives, we have implemented all three in the SPEED

[14] code, using the Shell [15] knock model for autoignition kinetics. Alternative (a) requires no special treatment. For the cutoff criterion in the alternative (b), we use the reaction rate, specifying cutoff when this exceeds 5%. This method is similar to that used by Natarajan et. al. [8], where temperature gradient is used as the criterion. Autoignition is considered to have occurred when the temperature rise exceeds $10^6 Ks^{-1}$ [9].

Our most extensive results, for which experimental data is available, cannot be shown here as they are commercially sensitive, but we can demonstrate all the major qualitative features using a 'standard' 4-valve pent-roof geometry. The chamber configuration and computational mesh are shown in fig. 1 and table 1 gives the engine starting fields and operating conditions.

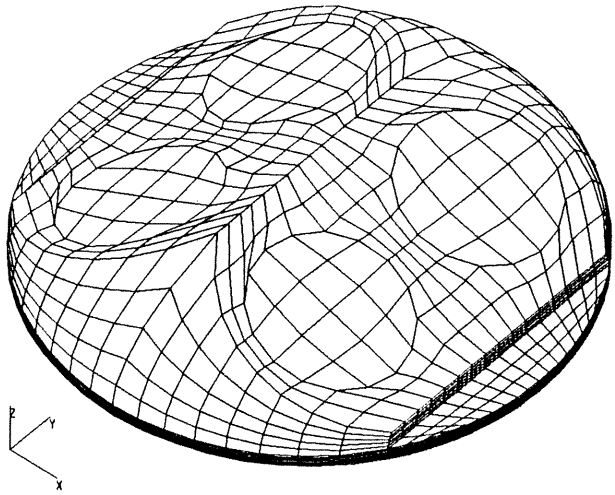

Fig. 1. Illustration of four-valve pent-roof combustion chamber and computational mesh, near TDC.

Except within the ODE system for knock chemistry, the SPEED code is fully implicit, giving fast run times, while the code structure has ensured easy insertion of alternative calculation methods into the coding. It should be noted that the value of the implicitness is wholly in the calculation of the compression flowfield and early combustion: to resolve the details of knock, the timestep was reduced to 0.1° CA.

The cylinder mean reaction rate and pressure time traces generated with the three models are shown in figs. 2 and 3 respectively. The ensemble-average calculation suffers from the well-established problem that the low-temperature kinetics accelerate the flame propagation, due to the Magnussen model's use of fuel depletion to characterize its reaction zone. Knock is also predicted too early due to the rise in average temperature produced by the flame and then suppressed by the accelerated propagation into the knock region. This leads to reaction-rate spikes corresponding to the knock initation/suppression cycles progressing with the flame. The two-phase model eliminates these effects and correctly predicts a single pressure peak corresponding to the onset of the large 'spike' in the global reaction rate due to

Table 1

4-valve Pent-Roof engine geometry and operating conditions

Bore :	80mm
Stroke :	80mm
Conecting rod length :	363.5mm
Compression Ratio :	9.74
Swept Volume :	402.1cc
Fuel :	90 PRF
Air fuel ratio :	13.344
Ignition Timing :	37° BTDC
Inlet valve closure :	130° BTDC
Piston temperature :	523 K
Liner temperature :	430 K

Bulk gas properties at inlet valve closure:
(imposed by reference to experimental data for a similar engine with same operating conditions)

Temperature :	310 K
Pressure :	1.0 bar
u' :	4.7 m/s
Dissipation rate :	1750.0 m^2/s^3
Swirl number :	1.1 (solid body)

'auto-ignition' of the end gas. By contrast, the interface criterion suppresses knock altogether in this calculation by switching off the low-temperature kinetics too soon. In this model, fine tuning of the cutoff can produce physically reasonable results, but at a cost of removing the predictive value of such calculations. The two-phase model predicts knock at 19.49° ATDC, a reasonable value for the operating conditions [18]. The cylinder average pressure traces do not exhibit the high frequency oscillations found in experimental results [18], attributed to shock waves picked-up as local pressure peaks by pressure transducers.

Fig. 4 shows the swirl flow and ensemble-averaged temperature fields on a diametral plane just below the squish surface, which is the plane in which knock is first observed, shortly before knock at 11.0° ATDC. The rotational symmetry of the calculation permits placing the two half-chamber views of this cut back-to-back in this way. The temperature field gives an impression of the probability distribution of the flame, with the elongated shape and skewed orientation due to the interaction between swirl and geometry, as seen from the velocity field. Fig. 5 shows the unburnt temperature field before and after knock has commenced, at 11.0° ATDC and 19.49° ATDC respectively, in the same manner. The position of the peak in the unburnt gas temperature before knock results from heat transfer from the wall during compression until compression heating reverses this process: this gives a peak some distance from the wall. The swirl accounts for the break of this otherwise

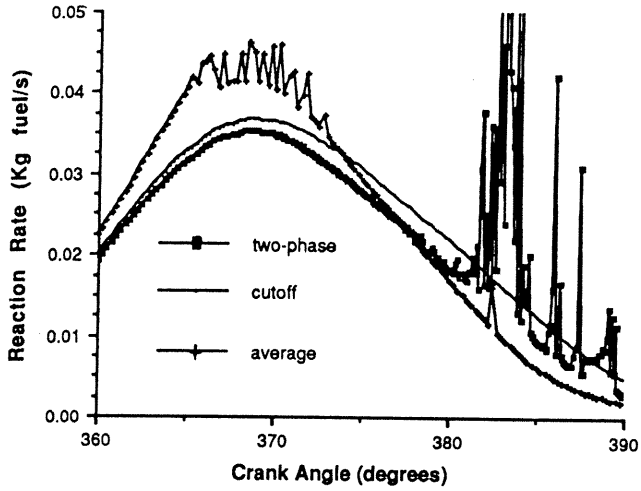

Fig. 2. Cylinder-mean fuel consumption rate vs. crank angle.

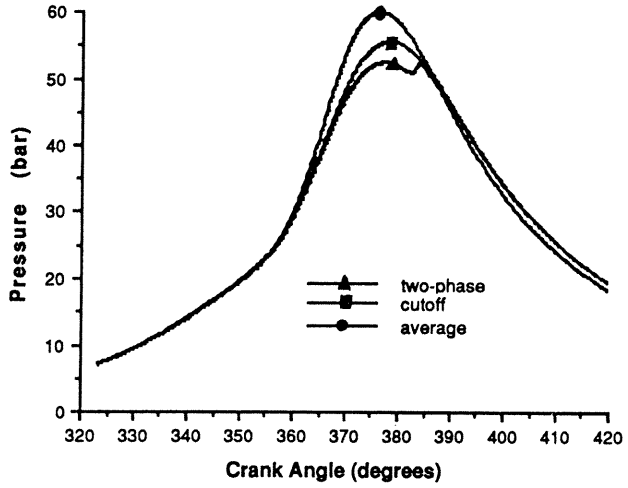

Fig. 3. Cylinder-mean pressure vs. crank angle.

toroidal maximum into two parts. The onset of knock also occures at this location as can seen from the unburnt gas temperature distribution after knock, indicating that wall heat transfer is an important factor in determining the location and timing of knock.

The unburnt gas concentration for total radicals 'R' of the Shell [15] reaction scheme before and after knock is shown in fig. 6 for the same times: the peak in the concentration correlates with the mesh cells where knock is first detected. The total degenerate branching agent 'B' (not shown) changes dramatically on autoignition: beforehand it was proportional to the unburnt fuel concentration, but immediately after, the minima have become maxima. This behaviour is typical of the two-stage end-gas ignition where R and B concentrations fall, indicating the presence of a cool flame, followed by a rapid rise as the end-gas ignites [10, 15].

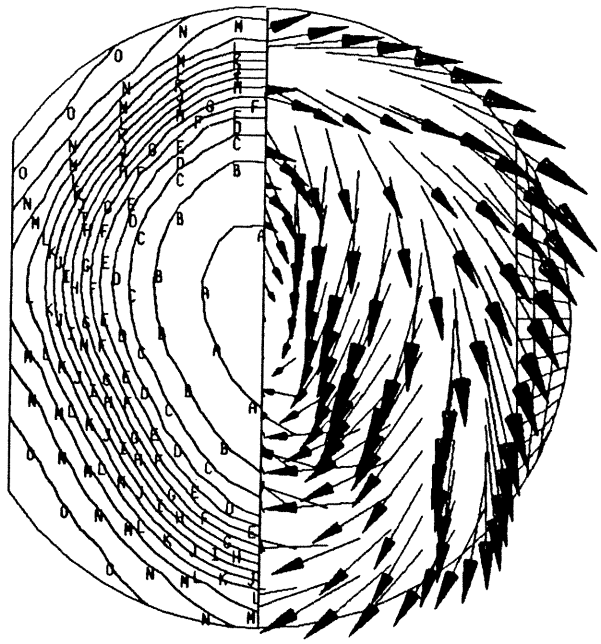

Fig. 4. Temperature contours and velocity vectors on a diametral plane just below the squish surface, at 11° ATDC. Contours are equi-spaced with A=2903K and O=949K. Velocity vector ——▶ =10.0 m/s.

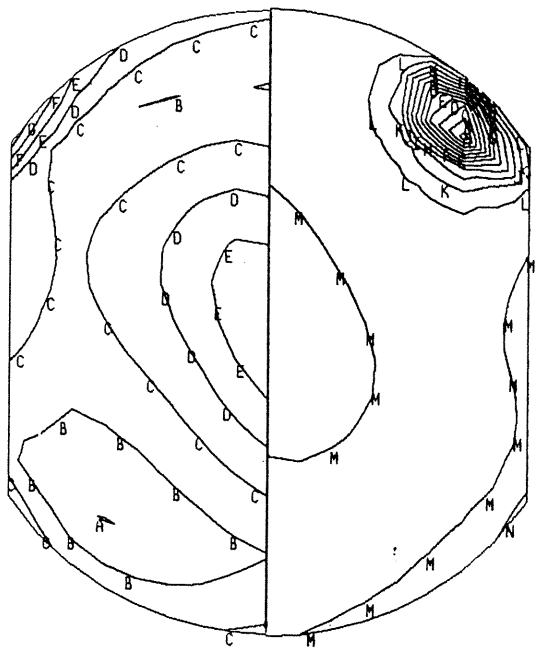

Fig. 5. Unburnt gas temperature contours on a diametral plane just below the squish surface.
Contours are equi-spaced.
Left section : 11.0° ATDC, A=888K, O=861K.
Right section : 19.49° ATDC, A=923K, O=799K.

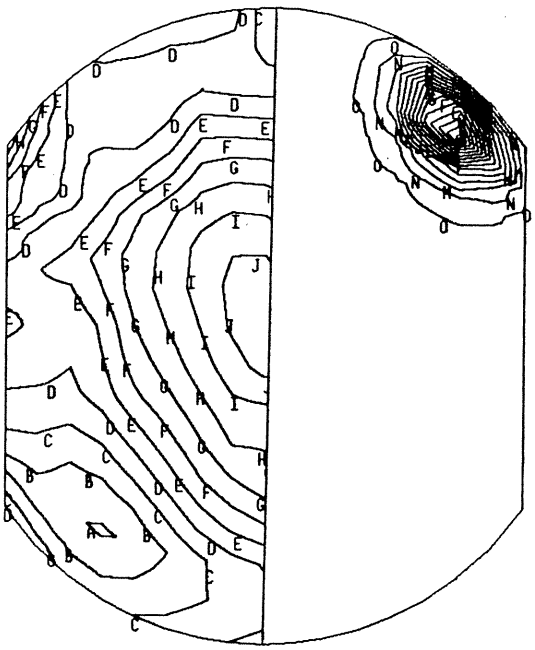

Fig. 6. Total radicals 'R' concentration contours on a diametral plane just below the squish surface. Contours are equi-spaced.
Left section: 11.0° ATDC, A=0.808, O=0.644ppm.
Right section: 19.49° ATDC, A=403, O=15.8ppm.

4. CONCLUSIONS

Using a two-phase representation of the mixture of burnt and unburnt gas in the laminar flamelet combustion regime, we have been able to obtain the correct qualitative behaviour for autoignition in a generic 4-valve pent-roof spark-ignition engine geometry, in conditions where single-phase ensemble average calculations give either early knock, or suppress it altogether. No special assumptions or modelling parameter sizes were required. These results are borne out by comparison with unpublished commercial experimental data, which show that the present method gives good prediction of both timing and position of knock. The equations are sufficiently simple to be incorporated into standard engine codes such as SPEED, since they do not require any major modifications to the code algorithm or data structures and so are intended to form a useful improvement to the multidimensional methodology in engine performance prediction.

REFERENCES

1. Bray, K.N.C., Libby, P.A., Moss, J.B., "Unified Modelling Approach for Premixed Turbulent Combustion-Part I: General Formulation", Combustion and Flames, Vol. 61: pp. 87-102, 1985.
2. Pope, S.B. and Cheng, W.K. : Twenty-Second Symposium (International) on Combustion, The Combustion Institute, p.781, 1989.
3. Veynante, D., Lacas, F., Maistret, E., and Candel, S.M.: Seventh Symposium on Turbulent Shear Flows, P. 26.2.1, 1989.
4. Cant, R.S., Pope, S.B., and Bray, K.N.C.: Twenty-Third Symposium (International) on Combustion, The Combustion Instiute, 1990.
5. Weller, H.G., Marooney, C.J. and Gosman, A.D.: Twenty-Third Symposium (International) on Combustion, The Combustion Institute, 1990.
6. Franke, C. and Peters, N.:Project Report SFB "Motorische Verbrennung" Projekt A2, Institut fur Technische Mechanik, RWTH Aachen, 1989.
7. Schapertons, H., Gupta, H. C., and Lee, W., Int. Symp. on Knocking of Combustion Engines, Wolfsburg, West Germany, 1981.
8. Natarajan, B., M.S.E. Thesis No. 1611-T, Princeton University, 1983.
9. Natarajan, B. and Bracco, F. V. Combustion and Flame 57: 179 - 197, 1984.
10. Hirst, S. L., and Krisch, L. J. , in Combustion Modeling in Reciprocating Engines (Mattavi and Amann, Eds.), Plenum, New York, pp. 193-229, 1980.
11. Male, T., Third Symposium on Combustion Flame and Explosion Phenomena, Williams and Wilkins, Baltimore, MD, pp. 721-726, 1949.
12. Lewis, B., and von Elbe, G., Combustion, Flames and Explosions of Gases, Academic Press, New York, 1961.
13. Magnussen, B.F. and Hjertager, B.H.: Sixteenth Symposium (International) on Combustion, The Combustion Institute,p. 1657, 1977.
14. Gosman A D and Marooney C J, IMechE, Autotech, Birmingham, 1989.
15. Halstead, M. P., Kirsch, L. J., and Quinn, C. P., Combustion and Flame 30 : 45-60, 1977.
16. Jones W.P., Models for Turbulent Flows with Variable Density and Combustion; "Prediction Methods for Turbulent Flow", Ed. Kollman W, Hemisphere Pub. Co, p. 379, 1980.
17. Libby P.A. and Williams F.A., "Turbulent Reacting Flows", Springer-Verlag, 1980.
18. Cuttler, D.H. and Giris, N.S., "Photography of Combustion During Knocking Cycles in Disc and Compact Chambers", SAE Technical Paper Series 880195, 1988.